860 J. Am. Chem. Soc. 1993, 115, 860–867

Nonlinear Optical Analysis of a Series of Triblock Copolymers Containing Model Polyenes: The Dependence of Hyperpolarizability on Conjugation Length

G. S. W. Craig,[†] R. E. Cohen,*,[†] R. R. Schrock,[‡] R. J. Silbey,[‡] G. Puccetti,[§] I. Ledoux,[§] and J. Zyss[§]

Contribution from the Departments of Chemical Engineering and Chemistry, Massachusetts Institute of Technology, Cambridge, Massachusetts 02139, and Centre National d'Etudes des Télécommunications (LA CNRS 250), 196, avenue Henri Ravera, 92220 Bagneux, France.

Received July 29, 1992

Abstract: Sequential ring-opening metathesis polymerization of norbornene and 7,8-bis(trifluoromethyl)tricyclo[4.2.2.0^{2,5}]-deca-3,7,9-triene with $Mo(CHCMe_3)(NAr)(OCMe_3)_2$ (Ar = 2,6-diisopropylphenyl) followed by linking termination with a conjugated dialdehyde results in highly soluble A–B–A triblock copolymers containing an oligomer of a precursor of Durham polyacetylene as the central block. Subsequent heat treatment converts the polyacetylene precursors into model polyenes. A series of these copolymers that had conjugation lengths ranging from 4 to 16 double bonds was synthesized. The polyenes were isomerized to the predominantly all-trans isomer. The presence of the polynorbornene chains solubilizes the polyenes, allowing their hyperpolarizability to be probed with electric field induced second harmonic generation; $\gamma_N(-2\omega;\omega,\omega,0)$ and $\gamma_N(0)$ varied with conjugation length to the 3.6 and 3.2 powers, respectively.

Introduction

There has been a significant amount of research on the nonlinear optical (NLO) behavior of organic molecules and polymers. This research has been driven both by interest in using organic materials in NLO devices and by the desire to understand the molecular and electronic processes that create NLO effects in these materials. Organic materials may prove useful in NLO devices because of their relatively large nonresonant optical nonlinearity and their sub-picosecond response time.[1-4] Moreover, organic NLO materials should be inexpensive and easy to fabricate compared to their inorganic counterparts, such as single crystals of $LiNbO_3$.[5,6] Applications of these molecules would utilize a variety of NLO effects, including second and third harmonic generation,[7] optical bistability,[8,9] and phase conjugation.[10]

The second- and third-order NLO effects are characterized by the bulk susceptibilities, $\chi^{(2)}$ and $\chi^{(3)}$, respectively, on the macroscopic level and the first and second hyperpolarizabilities, β and γ, on the molecular level. These effects have been studied for a vast array of organic molecules and polymers.[11,12] In all of these molecules, the magnitude of the hyperpolarizability depends on the extent of π electron conjugation. Thus, a firm knowledge of the relationship between the molecular hyperpolarizabilities and the π electron conjugation length is necessary for the scientific development of new NLO organic materials, the study of existing NLO materials, and the enhanced understanding of the electronic origin of NLO behavior.

It is expected that β and γ vary exponentially with conjugation length, N, in the form $\beta \propto N^{\alpha_1}$ and $\gamma \propto N^{\alpha_2}$. A number of theories have been used to predict values of the exponent α_2 ranging from 3 to 5.4.[13-19] These theories focus on the most basic conjugated system: the all-trans polyene. Experimental verification of these theoretical predictions has been difficult because of the crystallinity and virtual insolubility of polyenes having more than six double bonds. In the solid state, crystallinity prevents optical studies.[20] NLO studies of model polyenes in solution inevitably have a large systematic error because solubilities of long model polyenes are on the order of milligrams per liter.[21]

Because of the problematic physical properties of polyenes, experimentalists have instead examined soluble, substituted polyenes such as thiophene oligomers,[18] asymmetric donor–acceptor polyenes,[22] or retinols and carotenes.[23] Experimental determinations of α_1 and α_2 were performed.[22,24] However, none of these molecules is an unsubstituted, all-trans polyene that theorists study in their models. It is uncertain how the presence of the heteroatoms, substituents, or electron donors and acceptors would affect the NLO models.

In this article, we present a method of solubilizing polyenes that preserves their model nature. Triblock copolymers of polynorbornene–polyene–polynorbornene were synthesized, e.g., the co-

---

[†] Department of Chemical Engineering, Massachusetts Institute of Technology.

[‡] Department of Chemistry, Massachusetts Institute of Technology.

[§] Centre National d'Etudes des Télécommunications.

(1) Williams, D. J. *Angew. Chem., Int. Ed. Engl.* **1984**, *23*, 690.

(2) Prasad, P. N. In *Nonlinear Optical and Electroactive Polymers*; Prasad, P. N., Ulrich, D. R., Eds.; Plenum Press: New York, 1987; p 41.

(3) Kobayashi, T.; Hattori, T.; Terasaki, A.; Kurokawa, K. In *Nonlinear Optical and Electroactive Polymers*; Prasad, P. N., Ulrich, D. R., Eds.; Plenum Press: New York, 1987; p 137.

(4) Zyss, J.; Chemla, D. S. In *Nonlinear Optical Properties of Organic Molecules and Crystals*; Chemla, D. S., Zyss, J., Eds.; Academic Press: Orlando, FL, 1987; Vol. 1, p 23.

(5) Lytel, R.; Lipscomb, G. F.; Thackara, J.; Altman, J.; Elizondo, P.; Stiller, M.; Sullivan, B. In *Nonlinear Optical and Electroactive Polymers*; Prasad, P. N., Ulrich, D. R., Eds.; Plenum Press: New York, 1987; p 415.

(6) Nicoud, J. F.; Ledoux, I.; Zyss, J. *Molecular Nonlinear Optical Materials: Physics and Devices*; Academic Press: Orlando, FL, in press.

(7) Williams, D. In *Electronic and Photonic Applications of Polymers*; 218th ed.; Bowden, M. J., Turner, S. R., Eds.; American Chemical Society: Washington, D.C., 1988.

(8) Hunsperger, R. G. *Integrated Optics: Theory and Technology*, 2nd ed.; Springer-Verlag: New York, 1984; p 127.

(9) Ulrich, D. R. *Mol. Cryst. Liq. Cryst.* **1990**, *189*, 3.

(10) Pepper, D. M. *Sci. Am.* **1986**, *254*, 74.

(11) Levine, B. F.; Bethea, C. G. *J. Chem. Phys.* **1975**, *63*, 2666.

(12) Prasad, P. N.; Williams, D. J. *Introduction to Nonlinear Optical Effects in Molecules and Polymers*; 1st ed.; John Wiley and Sons, Inc.: New York, 1991; p 132.

(13) Zamani-Khamiri, O.; Hameka, H. F. *J. Chem. Phys.* **1980**, *73*, 5693.

(14) Soos, Z. G.; Ramasesha, S. *J. Chem. Phys.* **1989**, *90*, 1067.

(15) Pierce, B. M. *J. Chem. Phys.* **1989**, *91*, 791.

(16) de Melo, C. P.; Silbey, R. J. *J. Chem. Phys.* **1988**, *88*, 2567.

(17) Chopra, P.; Carlacci, L.; King, H. F.; Prasad, P. N. *J. Phys. Chem.* **1989**, *93*, 7120.

(18) Zhao, M. T.; Singh, B. P.; Prasad, P. N. *J. Chem. Phys.* **1988**, *89*, 5535.

(19) Beratan, D. N.; Onuchic, J. N.; Perry, J. W. *J. Phys. Chem.* **1987**, *91*, 2696.

(20) Meth, J. Personal communication.

(21) Puccetti, G.; Ledoux, I.; Zyss, J.; Blanchard-Desce, M.; Lehn, J. M. Manuscript in preparation.

(22) Messier, J.; Kajzar, F.; Sentein, C.; Barzoukas, M.; Blanchard-Desce, M.; Lehn, J. M.; Zyss, J. *Nonlinear Opt.*, in press.

(23) Hermann, J. P.; Ducuing, J. *J. Appl. Phys.* **1974**, *45*, 5100.

(24) Barzoukas, M.; Blanchard-Desce, M.; Josse, D.; Lehn, Y. M.; Zyss, J. *Chem. Phys.* **1989**, *133*, 323.

0002-7863/93/1515-860$04.00/0

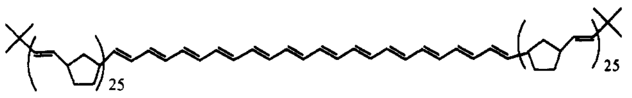

Figure 1. Polynorbornene–polyene–polynorbornene triblock copolymer **12t**.

polymer shown in Figure 1. The copolymers are synthesized in a relatively straightforward manner, using ring-opening metathesis polymerization (ROMP) with a molybdenum alkylidene initiator,[25] norbornene, and a Durham polyacetylene precursor monomer.[26] The highly soluble polynorbornene blocks effectively drag the polyene in the center block into solution, permitting the NLO properties of the model polyenes to be examined. A series of polyenes with increasing conjugation lengths was polymerized, isomerized, and subsequently examined with UV/vis spectroscopy and electronic field induced second harmonic generation (EFISH) to characterize the dependence of hyperpolarizability on conjugation length.

Copolymer Synthesis

General Procedures. All syntheses were performed under a nitrogen atmosphere in a Vacuum Atmosphere dry box or by using standard Schlenk/vacuum line techniques. Tetrahydrofuran (THF) was degassed, stirred over sodium/potassium alloy (Na/K) until the solvent turned blue, and then vacuum transferred immediately before use. Toluene for polymerizations was distilled over sodium and then stored over Na/K under nitrogen, and it was filtered and degassed prior to use. Methylene chloride was distilled from calcium hydride and stored over molecular sieves. Pivaldehyde was distilled twice from calcium hydride, degassed, and stored over nitrogen at −40 °C. Norbornene (**2**) was purified by distillation over sodium. $Mo(CHCMe_3)(NAr)(OCMe_3)_2$ (Ar = 2,6-diisopropylphenyl) (**1**),[27] 7,8-bis(trifluoromethyl)tricyclo-[4.2.2.0^{2,5}]deca-3,7,9-triene (**3**),[28] hexa-2,4-diene-1,6-dial (**4d**),[29] and octa-2,4,6-triene-1,8-dial (**5d**)[30,31] were synthesized according to literature procedures. Compound **4d** had to be extracted with cold toluene and resublimed to remove reaction byproducts such as **5d** and longer polyene dialdehydes.

Synthetic Method. All polymers were synthesized by ring-opening metathesis polymerization (ROMP) using initiator **1**. This initiator has been shown to yield homopolymers of **2** that have a very narrow molecular weight distribution.[25] Unlike its tungsten alkylidene analogs, **1** reacts with an aldehyde to form only the trans olefin.[32,33] **2** was used to form the solubilizing blocks because of the high solubility of polynorbornene. The polyene precursor monomer **3** was used because it was sufficiently stable at room temperature, it quickly converted to the polyene under mild conditions (120 °C, 5 min), and it was easy to synthesize relative to other Durham polyacetylene precursor molecules.

All of the copolymers studied here have the same basic structure: $[2]_{25}$–polyene–$[2]_{25}$. The subscript refers to the number of equivalents added during the polymerization; the actual block lengths may vary. Also, the sample numbers **6**–**13** refer to the conjugation length that the triblock copolymers would have if **3** polymerized stoichiometrically to yield only one specific conjugation length.

The linking copolymerization of **12**, diagrammed in Figure 2, is presented as an example of the polymerization technique. A solution of **1** (488 mg, 0.51 mmol) in 1.000 mL of toluene was injected into a solution of **2** (1207 mg, 12.82 mmol) in 24.000 mL of toluene at room temperature, and the mixture was stirred for 5 min. At this point an aliquot (0.343 mL of solution) of the living homopolymer (**LH**) was withdrawn from the reaction and terminated with a 10-fold excess of pivaldehyde. This solution was filtered through a 2-in. column of activated alumina to remove the deactivated initiator and set aside for GPC analysis. Two equivalents of **3** (269 mg, 1.01 mmol) in 5.343 mL of toluene was added to the **LH** solution and stirred for 25 min. An aliquot (0.352 mL of solution) of the living diblock copolymer (**LD-2**) was withdrawn and treated in the same manner as the **LH** aliquot. The linking termination was accomplished by adding a solution of **4d** (27.5 mg, 0.250 mmol) in 27 mL of toluene to the **LD-2** solution and stirring for 25 min. Finally, to drive the linking reaction to completion, the solvent was removed in vacuo. The resulting precursor polymer (**P-12**) was dissolved in 10 mL of methylene chloride. Initiator residue was removed by precipitating the polymer by dropwise addition of the methylene chloride solution to cold methanol. The polymer was collected on a glass frit, washed with cold methanol, dried under vacuum, and redissolved in 8 mL of toluene under nitrogen. This solution was placed in a pressure vessel and heated to 120 °C for 5 min, during which time the color changed from yellow-orange to deep red. The color change was evidence that the heating process converted **P-12** to **12** via a retro-Diels–Alder elimination of bis(trifluoromethyl)benzene. The pressure apparatus was cooled in an ice bath, and the polymer was precipitated in methanol as described above to remove bis(trifluoromethyl)benzene and any remaining traces of deactivated initiator, dried in vacuo, and stored under nitrogen at −40 °C. At this point, the polyenes in **12** are in an alternating trans(cis–trans)$_x$ isomeric state, with the exception of the two central trans double bonds, as shown in Figure 2.

The polyenes in **12** were converted to the predominantly all-trans form, **12t**, by exposure to medium-intensity UV/vis light, obtained from an Oriel Model 66002 mercury arc lamp. After the quality of **12** had been verified with GPC and UV/vis analysis, one-half of the polymer was dissolved in 10 mL of degassed methylene chloride under nitrogen in a sealed Pyrex pressure tube and illuminated with UV/vis light in a room temperature water bath under a mercury lamp for 2 days. A Schott WG 345 filter (~50% absorption at 345 nm) was used to prevent photodegradation of the polyenes. The room-temperature water bath and a 1-cm layer of water in a Pyrex Petri dish were used to prevent thermal degradation of the polyenes during illumination.

A few aspects of this polymerization technique deserve special attention. First, the linking termination of **LH** with dialdehyde **4d** or **5d** will yield triblock copolymer **4t** or **5t** that contains only 4-ene or 5-ene, respectively. The 4-ene and 5-ene are the all-trans isomers. To synthesize longer polyenes in the middle block, up to 2 equiv of **3** was used. Each additional equivalent of **3** adds four double bonds to the polyene in the final polymer. The polymerization of **3** results in a statistical distribution of polyene lengths. For example, the UV/vis spectrum of **12** suggests that a distribution of 8-enes, 10-enes, 12-enes, 14-enes, and 16-enes is present in the sample.

Copolymer Characterization

Experimental Apparatus. Gel permeation chromatographic (GPC) analysis was carried out at room temperature employing a Rheodyne Model 7125 sample injector, a Kratos Spectroflow 400 pump, Shodex KF-802.5, -803, -804, -805, and -800P columns, a Knauer differential refractometer, and a Spectroflow 757 absorbance detector on samples 0.1–0.3% w/v in THF that were filtered through a Millex-SR 0.5-μm filter in order to remove particulates. The GPC columns were calibrated versus commercially available polystyrene standards (Polymer Laboratories Ltd.) ranging from 1206 to 1.03 × 10^6 g/mol. Molecular weights (M_n) represent the molecular weight of a polystyrene standard that would elute in the same volume element as the polymer under consideration.

The UV/vis spectra were measured at room temperature on a Hewlett-Packard 8452A in-line diode array spectrophotometer.

---

(25) Schrock, R. R. *Acc. Chem. Res.* **1990**, *24*, 158.

(26) Edwards, J. H.; Feast, W. J.; Bott, D. C. *Polymer* **1984**, *25*, 395.

(27) Schrock, R. R.; Murdzek, J. S.; Bazan, G. C.; Robbins, J.; DiMare, M.; O'Regan, M. *J. Am. Chem. Soc.* **1990**, *112*, 3875.

(28) Bursics, A. R. L.; Bursics-Szekeres, E.; Murray, M.; Stone, F. G. A. *J. Fluorine Chem.* **1975**, *7*, 619.

(29) Kossmehl, G.; Bohn, B. *Chem. Ber.* **1974**, *107*, 710.

(30) Cope, A. C.; Nelson, N. A.; Smith, D. A. *J. Am. Chem. Soc.* **1954**, *76*, 1100.

(31) Anet, R. *Tetrahedron Lett.* **1961**, *20*, 720.

(32) Murdzek, J. S.; Schrock, R. R. *Organometallics* **1987**, *6*, 1373.

(33) Sankaran, V. Unpublished results.

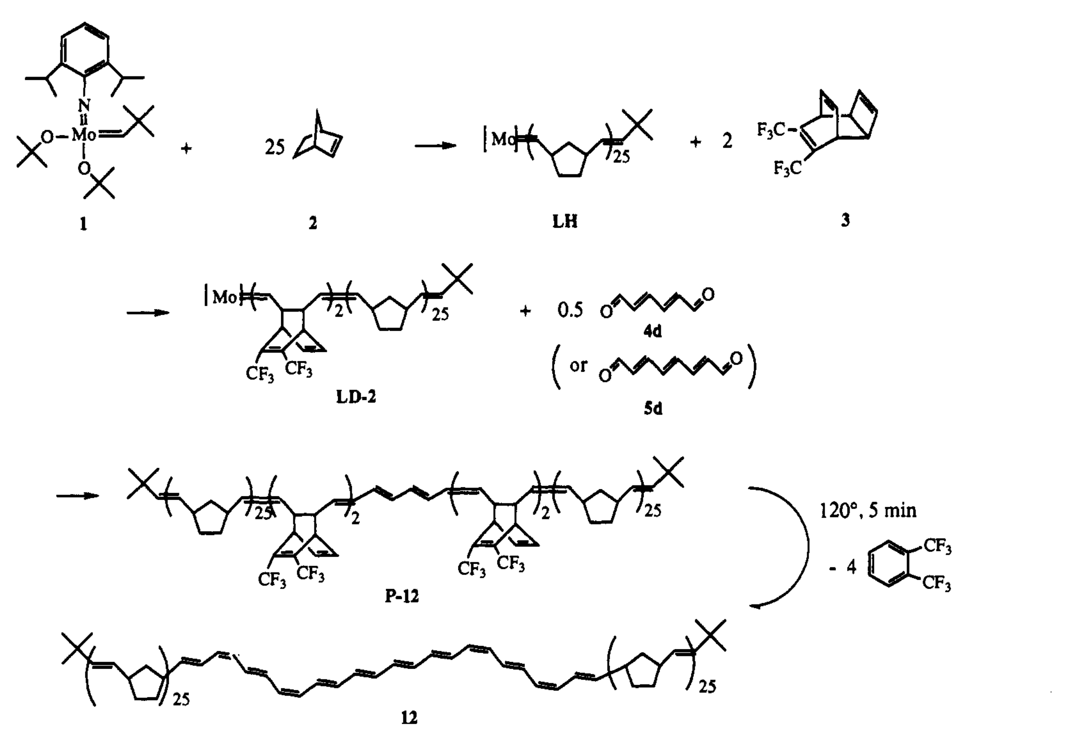

Figure 2. Example of linking copolymerization route to triblock copolymer **12**. Use of dialdehyde **5d** instead of **4d** would yield **13**.

Solutions were analyzed in a quartz cuvette and had concentrations in the range 25–100 mg/L. Spectra were taken in the solid state, in THF, and in methylene chloride.

Determination of Polyene Distribution. The final copolymers, **6–13**, and their corresponding predominantly all-trans isomers, **6t–13t**, contained a distribution of either even or odd polyenes. It was necessary to characterize this distribution in order to determine the contribution of each polyene to the effective hyperpolarizability of a given copolymer. This was accomplished by a deconvolution of the UV/vis spectra of the polyenes in the copolymers, described in detail in the Appendix. Similar to a previous study of relatively short polyenes,[34] a theoretical approximation, consisting of a weighted summation of Gaussian functions, was developed to model the spectra of a series hypothetical polynorbornene-capped polyenes. The theoretical polyene spectra were fit to the copolymer spectra with an implementation of the Nelder–Meade simplex algorithm.[35]

Electronic Field Induced Second Harmonic Generation. The standard EFISH technique was used for measurements of the third-order polarizabilities of polyenes. The fundamental wavelength was emitted at 1.34 μm by a Q-switched, mode-locked Nd^{3+}:YAG laser, providing pulse trains of about a 90-ns envelope duration (individual pulses of 160-ps duration). The repetition rate was 10 Hz. The second harmonic (SH) signal was measured, pulse per pulse, by a sampling integrator device and recorded. Each SH pulse intensity was divided by a standard second harmonic signal emitted by illumination of a highly nonlinear powder (*N*-(4-nitrophenyl)-L-prolinol) by a small part of the incident fundamental beam, in order to rule out fluctuations in laser intensity. The reference was the pure solvent THF.

EFISH measurements were performed at three different concentrations of copolymer in THF. The third-order susceptibility, $\Gamma^{2\omega}(0)$, of THF was determined at 1.34 μm by relative measurements using chloroform as a reference. $\Gamma^{2\omega}(0)$ of THF equals 0.67×10^{-14} esu.

$\Gamma^{2\omega}(0)$ of THF was analyzed before and after each copolymer analysis to verify the constancy of the apparatus. The hyperpolarizability of a sample of polynorbornene homopolymer was analyzed to determine the effect of the polynorbornene chains on the hyperpolarizability of the copolymer. Another sample of polynorbornene was washed with 1% NaOH to remove any residual traces of deactivated initiator. This clean sample was analyzed and compared with the polynorbornene sample that had been precipitated, but not washed, to determine whether traces of the initiator would affect the EFISH measurements.

The method for converting the second harmonic intensity and the interference pattern data of EFISH into a macroscopic cubic susceptibility Γ has been presented previously in the literature.[36,37] From the Γ value we can infer the microscopic third-order polarizabilities of the nonlinear molecules assuming, in an EFISH experiment, that the orientational (second-order) contribution $(\mu\beta/5kT)$ equals zero. It is customary to assume that the susceptibility of the solution is the sum of the susceptibilities of the various species contained on it.[38,39] Γ is frequency and concentration dependent. For the sake of simplicity, we will write

$$\Gamma(-2\omega;\omega,\omega,0) \equiv \Gamma^{2\omega}$$

and $\Gamma = \Gamma^0$ at $\omega = 0$. Therefore, for a given "nominal" polymer P in solution, the macroscopic cubic susceptibility $\Gamma_{\mathrm{P}}^{2\omega}$ is given by

$$\Gamma_{\mathrm{P}}^{2\omega} - \Gamma^{2\omega}(0) = c_{\mathrm{P}} f N_{\mathrm{Av}} \sum_{N_{\min}}^{N_{\max}} c_{\mathrm{P},N} \gamma'^{2\omega}_{N} \qquad (1)$$

where c_{P} is the molar concentration of the polymer, $c_{\mathrm{P},N}$ is the mole fraction of *N*-ene in sample P, f is the local field correction, N_{Av} is Avogadro's number, $\Gamma^{2\omega}(0)$ is the macroscopic susceptibility of the pure solvent, and

$$\gamma'^{2\omega}_{N} = \gamma_N^{2\omega} + \gamma_{\mathrm{nbe}}^{2\omega} \qquad (2)$$

where $\gamma_N^{2\omega}$ and $\gamma_{\mathrm{nbe}}^{2\omega}$ are the hyperpolarizabilities of the polyene N and the polynorbornene chains, respectively, at 2ω. Then eq 1 becomes

$$\Gamma_{\mathrm{P}}^{2\omega} - \Gamma^{2\omega}(0) - f N_{\mathrm{Av}} c_{\mathrm{P}} \gamma_{\mathrm{nbe}}^{2\omega} = c_{\mathrm{P}} f N_{\mathrm{Av}} \sum_{N_{\min}}^{N_{\max}} c_{\mathrm{P},N} \gamma_N^{2\omega} \qquad (3)$$

The frequency-dispersed $\gamma_N^{2\omega}$ values can be deduced from the

---

(34) Granville, M. F.; Kohler, B. E.; Snow, J. B. *J. Chem. Phys.* **1981**, *75*, 3765.

(35) *MathWorks PRO-MATLAB User's Guide*, 1st ed.; The MathWorks, Inc.: South Natick, MA, 1989.

(36) Bethea, C. G. *Appl. Opt.* **1975**, *14*, 1447.

(37) Oudar, J. L. *J. Chem. Phys.* **1977**, *67*, 446.

(38) Ledoux, I.; Zyss, J. *Chem. Phys.* **1982**, *73*, 203.

(39) Kajzar, F.; Ledoux, I.; Zyss, J. *Phys. Rev. A* **1987**, *36*, 2210.

Table I. Results of GPC Analysis of Copolymers

copolymer sample	polydispersity	calcd precursor M_n	calcd M_n	GPC M_n
H	1.06	4814	4814	7000
4	1.09	4918	4918	8900
5	1.17	4944	4944	7900
6	1.10	5184	4970	8000
7	1.08	5210	4996	7400
8	1.15	5450	5022	9100
9	1.06	5476	5048	8700
10	1.08	5716	5074	7800
11	1.10	5742	5100	8200
12	1.07	5982	5126	8300
13	1.09	6008	5152	7700

experimental data for $\Gamma_P^{2\omega}$, $\Gamma^{2\omega}(0)$, $\gamma_{nbe}^{2\omega}$, c_P, and $c_{P,N}$. For the sake of comparison, a "$\gamma_P^{2\omega}$", corresponding to the effective hyperpolarizability of the distribution of polyene lengths, can be defined as

$$\gamma_P^{2\omega} = \frac{(\Gamma_P^{2\omega}(x) - \Gamma^{2\omega}(0))}{c_P f N_{Av}} \tag{4}$$

According to the previously mentioned models,[13-19] an experimental relationship between $\gamma_N^{2\omega}$ and N can be assumed:

$$\gamma_N^{2\omega} = \gamma_1^{2\omega} N^{\alpha_2} \tag{5}$$

The final values of $\gamma_1^{2\omega}$ and α_2 were determined by a two-parameter least-squares fit of the EFISH model to the data.[35]

By assuming a three-level model for γ in the nonresonant regime, in which the energy of the highest level is much larger than the energy of the fundamental wavelength (1.34 μm), the zero-frequency hyperpolarizability γ_N^0 of the N-ene can be found from[40]

$$\gamma_N^0 = \gamma_N^{2\omega}(1 - (\lambda_N/\lambda_f)^2)(1 - 4(\lambda_N/\lambda_f)^2) \tag{6}$$

where λ_N is the wavelength at maximum absorption of the N-ene and λ_f is the fundamental wavelength. A relationship between γ_N^0 and N similar to that in eq 5 can be assumed:

$$\gamma_N^0 = \gamma_1^0 N^{\alpha_2{}^0} \tag{7}$$

Results

Polymerization. Polymerization of the diblock copolymers of **2** and **3** has been reported in detail previously.[41] The linking copolymerization step had a negligible effect on the polydispersity of the triblock copolymer compared to an equivalent sequentially polymerized triblock copolymer. It was necessary to remove the solvent in vacuo to drive the linking reaction to completion. If the solvent was not removed, a second peak, corresponding to monoterminated diblock copolymer, appeared in the GPC scan of the copolymer. There was no evidence of polyene cross-linking in the triblock copolymers; the GPC scans of the triblock copolymers before and after the retro-Diels–Alder conversion of the poly **3** block to polyenes were virtually identical, except for an expected slight decrease in M_n after conversion.

In this work, GPC was used to examine qualitatively the polydispersity, X_m, of the triblock copolymers. The GPC scan of each copolymer consisted of one peak without any visible shoulders when 0.5 equiv of dialdehyde was added. As expected, the linking copolymerization method was sensitive to stoichiometry. When ~1.5 equiv of dialdehyde was used to terminate the polymerization, two distinct peaks, corresponding to mono- and dicapping, were observed.

As shown in Table I, the polydispersity of the triblock copolymers ranged from 1.06 to 1.17. The polystyrene-equivalent molecular weights of the precursor polymers were in the range of 7400–9100. When divided by the polystyrene/polynorbornene GPC conversion factor[44] of 2,[42] the GPC values were consistently lower than the calculated ones. However, the conversion factor applies only to polynorbornene homopolymer. The random coil of the precursor triblock copolymer, containing repeat units of **3** as well as a 4-ene or 5-ene segment, undoubtedly will differ from a random coil of polynorbornene.

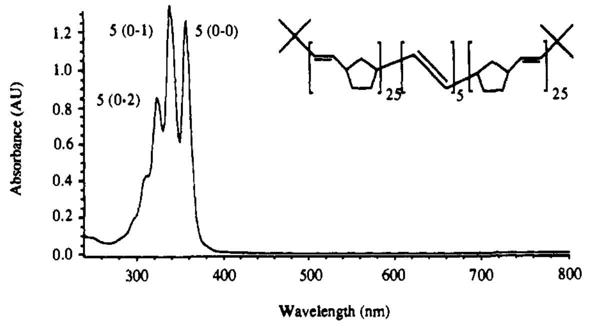

Figure 3. UV/vis spectrum of copolymer **5t** in methylene chloride. Numbers in parentheses identify the vibronic finger of the 5-ene $\pi\pi^*$ absorption band.

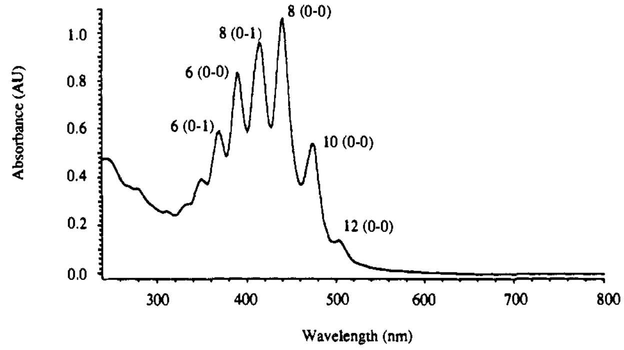

Figure 4. UV/vis spectrum of copolymer **8t** in methylene chloride. Numbers in parentheses identify the vibronic finger of the respective N-ene $\pi\pi^*$ absorption band.

UV/vis Spectroscopy. Copolymers **4t** and **5t** were white in color, while copolymers **P-6–P-13** were yellow. The yellow color of the precursor copolymers was evidence of short conjugated segments, ranging in size from 6-ene to 9-ene, in the central block. These polyenes were readily apparent in the spectra of **P-6–P-13**. The existence of these short polyene segments is apparently caused by the relative ease with which the **3** repeat unit adjacent to the initiator undergoes the Diels–Alder reaction.[43] There is sufficient time for the retro-Diels–Alder reaction during the linking step of the copolymerization. After conversion, the colors of the copolymers ranged from yellow (**6**) to orange (**9**) to deep red (**13**).

The dominant features in the UV/vis spectra of all of the copolymers were the vibronic fingers of the $\pi\pi^*$ absorption band. The spectra of copolymers **4t** or **5t** revealed that these two polymers contain only the 4-ene or 5-ene, respectively, as shown in Figure 3. The spectra for the copolymers containing longer polyenes, such as **8t** shown in Figure 4, showed that a distribution of polyenes was obtained, as anticipated in the synthesis section. In the copolymers that contained longer polyenes, such as **13** and **13t**, a second band of small peaks near 310 nm was observed. This absorption band was assigned to the $2^1B_u \leftarrow 1^1A_g$ transition, also observed in Knoll's study.[44] These trends were observed for both the as-synthesized alternating polyenes as well as the isomerized, predominantly all-trans polyenes.

The usual method of describing the relationship between the energy of the HOMO–LUMO transition and conjugation length for a series of polyenes in solution is with the equation $E_N = E_\infty$

---

(40) Ledoux, I.; Zyss, J.; Silbey, R. J. Manuscript in preparation.

(41) Krouse, S. A.; Schrock, R. R. *Macromolecules* **1988**, *21*, 1885.

(42) Sankaran, V.; Cohen, R. E.; Cummins, C. C.; Schrock, R. R. *Macromolecules* **1991**, *24*, 6664.

(43) Park, L. Y.; Stieglitz, S.; Crowe, W. E.; Schrock, R. R. *Macromolecules* **1991**, *24*, 3489.

(44) Knoll, K.; Schrock, R. R. *J. Am. Chem. Soc.* **1989**, *111*, 7989.

Table II. Polyene Mole Fractions in the Isomerized Copolymer Samples

	copolymer									
polyene mole fraction	4t	5t	6t	7t	8t	9t	10t	11t	12t	13t
$c_{P,4}$	1		0.320							
$c_{P,5}$		1		0.167						
$c_{P,6}$			0.382		0.196		0.063			
$c_{P,7}$				0.528		0.395		0.243		0.055
$c_{P,8}$			0.242		0.405		0.175		0.011	
$c_{P,9}$				0.224		0.353		0.243		0.105
$c_{P,10}$			0.050		0.304		0.44		0.275	
$c_{P,11}$				0.063		0.193		0.338		0.176
$c_{P,12}$			0.007		0.096		0.272		0.391	
$c_{P,13}$				0.018		0.059		0.158		0.477
$c_{P,14}$							0.050		0.240	
$c_{P,15}$								0.018		0.188
$c_{P,16}$									0.084	

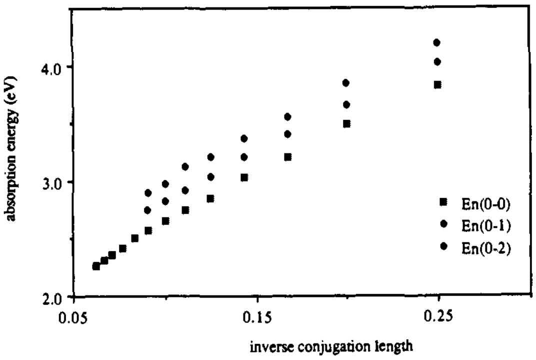

Figure 5. Absorption energy of the (0–0), (0–1), and (0–2) vibronic fingers of the $\pi\pi^*$ transition.

$+ k/N$, where E_N is the absorption energy at maximum absorption of a given N-ene, E_∞ is the absorption energy of a hypothetical infinite polyene, and k is a constant.[45] The fits of this equation to the energy at maximum absorption of the (0–0), (0–1), and (0–2) vibronic peaks of the alternating and predominantly all-trans isomers, shown in Figure 5, were very good. As in previous research,[44] the data for 4-ene and 5-ene were omitted in the determination of E_∞. E_∞ values for the $\pi\pi^*$ (0–0), (0–1), and (0–2) transitions of the alternating isomer in THF were 1.81, 1.98, and 2.17 eV, respectively. The corresponding values of the predominantly all-trans isomer were 1.72, 1.95, and 2.12 eV. In methylene chloride, the E_∞ values of the $\pi\pi^*$ (0–0) transition of the predominantly all-trans and alternating isomers were 1.75 and 1.83 eV, respectively. Inclusion of the $\lambda_{N,i}$ values of the predominantly all-trans 4-ene and 5-ene results in a good fit in which the E_∞ values were 1.79, 2.03, and 2.19.

If only the 6–11-ene data were used in the linear fit, E_∞ was 1.79 for the $\pi\pi^*$ (0–0) transition in THF. This indicates that the long ($n > 11$) polyene data skew the linear fit toward lower energy. The E_∞ determined from the 6–11-ene fit was appropriate for comparison with the E_∞ values of the $\pi\pi^*$ (0–1) and (0–2) transitions. The energy differences between the (0–0) and (0–1) and the (0–1) and (0–2) vibronic fingers of a hypothetical infinite polyene were 1320 and 1120 cm^{-1}, respectively.

The isomerization process was followed with UV/vis spectroscopy. After 2 h of isomerization of a copolymer in solution, changes in its spectrum were readily apparent. First, there was a 2–8-nm red shift of all of the vibronic fingers of a given polyene. Within a given polyene, the $\pi\pi^*$ (0–0) vibronic finger had the largest red shift. The shorter polyenes had a smaller red shift than the longer polyenes. This was expected because the short polyenes have fewer cis bonds relative to the number of trans bonds; the 8-ene, for example, has only two cis bonds and six trans bonds, whereas the 12-ene has four cis bonds and eight trans bonds. Second, the height of the (0–0) peak grew and the height of the (0–1) peak decreased. This result was expected because of the difference of the Franck–Condon effect between cis and trans polyenes. Finally, the vibronic fingers in the predominantly all-trans isomer were sharper and more well-defined than in the original alternating isomer. These changes asymptotically reached a limit within 1 day of UV exposure.

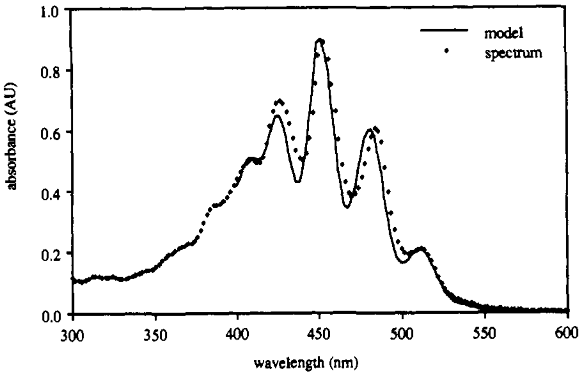

Figure 6. UV/vis spectrum of 11t and the corresponding model spectrum.

Table III. Effective Copolymer Hyperpolarizabilities of the Copolymers

	$\gamma_P^{2\omega}$ (10^{-36} esu)	
copolymer	alternating	isomerized
4		490
5		390
6	600	560
7	1100	1100
8	740	1100
9	1300	
10	1800	2100
11	2700	2600
12	3400	4100
13	4700	5100

The copolymer UV/vis absorption model fit the actual spectra very well, as seen in Figure 6. The polyene mole fractions, $c_{P,N}$, determined from the copolymer UV/vis spectra, are listed in Table II. The values of $c_{P,N}$ were used to determine the dependence of hyperpolarizability on polyene conjugation length.

Electronic Field Induced Second Harmonic Generation. The hyperpolarizability of the polynorbornene homopolymer (approximately 50 equiv) was 130 × 10^{-36} esu, regardless of whether the polymer was washed with 1% NaOH (aqueous) to remove traces of initiator. The hyperpolarizabilities for both the as-polymerized and the isomerized copolymers are presented in Table III. As expected, the $\gamma_P^{2\omega}$ increased exponentially with the nominal conjugation length, as seen in Figure 7. The exponents for the as-polymerized and the isomerized copolymers were 2.9 and 3.0, respectively.

The best fit of the model (eq 5 substituted into eq 3) to the EFISH data of the isomerized copolymers resulted in $\gamma_1^{2\omega}$ and α_2 of 0.49 × 10^{-36} esu and 3.6, respectively. The solid line of hy-

---

(45) Dale, J. *Acta Chem. Scand.* **1957**, *11*, 265.

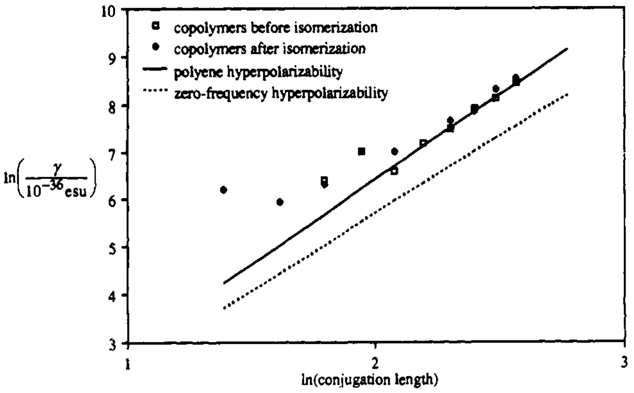

Figure 7. $\gamma_P^{2\omega}$ before and after isomerization, along with the values of $\gamma_N^{2\omega}$ and γ_N^0 for the individual model polyenes. The lines are not fit to the data shown; they are determined from the concentration deconvolution process and eqs 5 and 7, respectively. In the case of the copolymers, conjugation length refers to the copolymer sample number.

Table IV. Hyperpolarizabilities of Polyenes Calculated from Equations 5 and 6

polyene	$\gamma_N^{2\omega}$ (10^{-36} esu)	γ_N^0 (10^{-36} esu)	polyene	$\gamma_N^{2\omega}$ (10^{-36} esu)	γ_N^0 (10^{-36} esu)
4	68	50	**11**	2500	1100
5	150	99	**12**	3400	1500
6	290	180	**13**	4500	1900
7	500	280	**14**	5800	2400
8	800	400	**15**	7500	2900
9	1200	570	**16**	9400	3600
10	1800	830			

perpolarizabilities, $\gamma_N^{2\omega}$, of the *N*-enes shown in Figure 7 was determined from eq 5 with the derived values of $\gamma_1^{2\omega}$ and α_2. Equation 6 and the determined values of $\gamma_N^{2\omega}$ were used to calculate the corresponding γ_N^0; these hyperpolarizabilities are presented in Table IV. A value of λ_1 equal to 175 nm[46] was used in eq 6 to calculate $\gamma_1^0 = 0.45 \times 10^{-36}$ esu. Finally, the zero-frequency value of α_2 was 3.2, as determined from a linear fit of eq 7 to the values of γ_N^0 in Table IV with γ_1^0 fixed at 0.45×10^{-36} esu.

The validity of the three-level model for γ in the nonresonant regime was confirmed by comparison of the results from EFISH measurements at 1.34 μm and THF measurements at 1.91 μm. The hyperpolarizabilities obtained from these two different techniques give rise, after applications of a three-level model, to the same "static" $\gamma(0)$ values. The approximation is not general for all polyenes and frequencies; however, it was valid in this case.

Discussion

Triblock copolymers of **2** and **3** previously have been synthesized by ROMP with **1** by sequentially reacting the monomers with the initiator and then terminating the polymerization with an aldehyde such as pivaldehyde.[41] The linking copolymerization route presented here differs from the previous work only in its utilization of a conjugated dialdehyde to terminate the polymerization. The linking copolymerization route has several advantages over the sequential polymerization of triblock copolymers. First, linking copolymerization eliminates the possibility of premature termination, caused by impurities, during the polymerization of the third block. Linking termination also eliminates the possibility of the formation of isolated 3-enes in the third block of polynorbornene, a problem caused by the lower reactivity of **3** relative to **2** and encouraged in previous work.[41] As seen in Table II, each copolymer contained at most five different conjugation lengths.

The omission of the wavelengths at maximum absorption of the UV/vis spectra of **4t** and **5t**, defined as $\lambda_{4,i}$ and $\lambda_{5,i}$ in the Appendix, in the determination of E_∞ is debatable. The data for **4t** and **5t** were excluded primarily for the sake of comparison with the alternating isomers, of which there are no 4-enes or 5-enes, as well as with Knoll's data, which also omitted the shorter polyenes in the determination of E_∞. It has been shown that the $\pi\pi^*$ absorption energy of short polyenes varies with the inverse square root of conjugation length.[47] Additionally, the definition of E_∞ leads to the conclusion that it is more appropriate to omit data obtained from shorter polyenes. The better fit of the model of the copolymer spectra also seems to justify the exclusion of the **4t** and **5t** data from the determination of E_∞. When the $\lambda_{N,i}$ data of **4t** and **5t** were included in the fit of the higher ordered vibronic shifts, the fit of the model with the copolymer spectra was poor because the (0–1) and (0–2) vibronic fingers of the model did not coincide with the corresponding peaks in the actual spectra.

The energy difference between the (0–0) and the (0–1) vibronic states was in the range of 1600–1370 cm^{-1}, whereas the energy difference between the (0–1) and the (0–2) spanned 1310–1470 cm^{-1}, similar to previous polyene studies.[45,48] These energy differences approximately correspond to the ground-state carbon–carbon double-bond stretch of Durham polyacetylene observed[49] at 1470 cm^{-1}. The energy difference between vibronic states in the $\pi\pi^*$ transition decreased with increasing conjugation length, as previously observed.[47,50] For example, the (0–0) and (0–1) vibronic states in the 4-ene were separated by 1600 cm^{-1}; the difference decreased to 1470 cm^{-1} in the 8-ene.

A direct comparison of the absorption maxima and E_∞ of the polyenes examined here and those of Knoll's *tert*-butyl-capped polyenes was hindered by the insolubility of polynorbornene in pentane, the solvent used by Knoll. Knoll did analyze the predominantly all-trans 8-ene and 9-ene in methylene chloride, in which polynorbornene is very soluble. The $\lambda_{N,i}$ values of the vibronic fingers of the 8-ene and 9-ene in the triblock copolymers were red shifted by 6 and 8 nm, respectively. The red shift can be explained by the hyperconjugation effect upon the polyenes studied here, which are pseudo-isopropyl capped. A comparison of the ~350 cm^{-1} red shift caused by hyperconjugation in the 9-ene with the 890 cm^{-1} red shift of the 9-ene $\pi\pi^*$ (0–0) band relative to the corresponding band of the 8-ene shows that the hyperconjugation effect of each α-CH molecular orbital is equivalent to almost one-quarter of a double bond. In terms of E_∞, the values determined in this study, where only the 6–11-ene were considered, were virtually identical to those determined by Knoll. As expected, a comparison of E_∞ values of the alternating and predominantly all-trans polyenes in the copolymers reveals a decrease in band gap energy of the predominantly all-trans isomer.

The determination of the individual polyene concentrations in each of the triblock samples will be slightly in error due to the limited data and the approximations inherent in the construction of the empirical model (see the Appendix). The largest sources of error would be present in the concentrations of the longest and shortest polyenes. Extinction coefficient and $\lambda_{N,i}$ data of the longest polyenes had to be extrapolated from the data of the polyenes shorter than the 12-ene. The derived concentrations of the shortest polyenes also had a larger than normal errors because the model only accounts for the absorption of the first four vibronic states of the $\pi\pi^*$ transition. It does not account for the small, yet significant, absorption of each polyene at wavelengths shorter than the $\pi\pi^*$ absorption band. The absorption at short wavelengths is readily apparent in Knoll's spectra.

Despite its shortcomings, the model seems to be the most accurate method of empirically determining the molar concentrations of the polyenes in a copolymer while taking into account the Gaussian shape of the absorption bands of each vibronic finger of each polyene. Moreover, it should be noted that once the polyene spectra model parameters were determined, the only copolymer spectra model parameters varied to fit the actual co-

---

(46) Pavia, D. L.; Lampman, G. M.; Kriz, G. S. J. *Introduction to Spectroscopy*; Saunders College Publishing: Philadelphia, 1979; p 192.

(47) Sondheimer, F.; Ben-Efraim, D. A.; Wolovsky, R. *J. Am. Chem. Soc.* **1960**, *83*, 1675.

(48) Mebane, A. D. *J. Am. Chem. Soc.* **1952**, *74*, 5227.

(49) Shirikawa, H.; Ito, T.; Ikeda, S. *Polym. J.* (*Tokyo*) **1973**, *4*, 460.

(50) Rimai, L.; Heyde, M. E.; Gill, D. *J. Am. Chem. Soc.* **1973**, *95*, 4493.

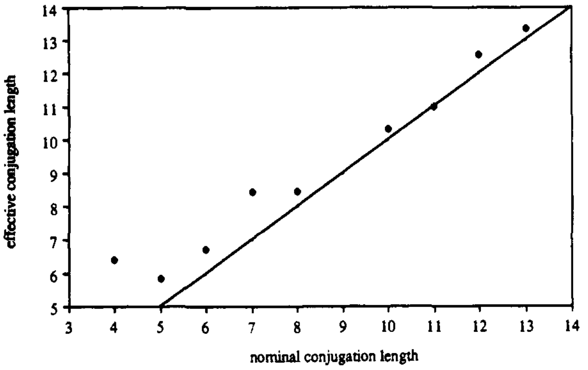

Figure 8. Comparison of the nominal conjugation length of a copolymer, corresponding to its sample number, and its effective conjugation length. The line of slope unity is drawn for reference.

polymer spectra were the polyene mole fractions, $c_{P,N}$. The extinction coefficients for all of the vibronic fingers were determined from Knoll's data. The $\lambda_{N,i}$ and w_N were determined from the copolymer spectra prior to the actual fit to determine the $c_{P,N}$.

Because of the imperfections inherent in the deconvolution of the UV/vis spectra and the derivation of the polyene concentrations in a given copolymer, the determination of α_2 is not flawless. However, the deconvolution process does give an idea of the difference between the nominal conjugation length of the polyene in a copolymer (i.e., 8 for sample **8**) and the effective conjugation length of the copolymer, as seen in Figure 8. For example, **8t** behaves as if it were a polyene with a conjugation length of 8.3 double bonds.

The difference in the $\gamma_P^{2\omega}$ value of the alternating polyene isomers and the predominantly all-trans isomer is relatively small. This small difference once again reflects the fact that the as-polymerized copolymers contain polyenes that already have a large trans content. For example, when **13** isomerizes to **13t**, only four double bonds isomerize from cis to trans.

Conclusions

Similar to previous work,[41] sequential ROMP of **2** and **3** with a molybdenum–alkylidene initiator proceeded in a living manner to yield diblock copolymers with very low polydispersities. Subsequent linking of the living diblock copolymer with a conjugated dialdehyde formed a triblock copolymer with low polydispersity and, importantly, no interruption in the conjugated sequence. The initiator permitted the synthesis of a series of copolymers whose polyene block had a relatively narrow conjugation length distribution. Each copolymer contained at most five different conjugation lengths, and the relative amounts of these species in each copolymer could be determined with reasonable accuracy.

The highly soluble polynorbornene chains solubilized the otherwise insoluble polyenes, thereby permitting examination of their hyperpolarizability. The effective hyperpolarizability of the copolymers at 1.34 μm varied with nominal conjugation length to the 2.9 and 3.0 powers in the case of the alternating and predominantly all-trans isomers, respectively. The exponents α_2 and α_2^0, reflecting the power law dependence of $\gamma^{2\pi}$ and γ^0 on conjugation length, were 3.6 and 3.2, respectively.

A more accurate evaluation of α_2 and α_2^0 could be determined if there were no distribution of conjugation lengths in any of the copolymers. We are currently synthesizing triblock copolymers containing discrete all-trans 9–12-enes for a more direct NLO analysis of the variation of hyperpolarizability with conjugation length.

Acknowledgment. We thank the National Science Foundation (Grant DMR 87-19217 through the MIT Center for Material Science and Engineering). R.R.S. thanks the Department of Energy for support of polyene research. G.S.W.C. thanks the National Science Foundation for a graduate fellowship, V. Sankaran for a generous supply of **3**, and N. Ferrier for helpful discussions regarding multivariable function minimization.

Appendix

Determination of Polyene Distribution. Deconvolution of the UV/vis spectra exclusively dealt with the absorption band associated with the promotion of a π electron from the highest occupied molecular orbital (HOMO) to the lowest unoccupied molecular orbital (LUMO), also known as the $1^1B_u \leftarrow 1^1A_g$ or the $\pi\pi^*$ transition. Similar to the results of previous research, the HOMO–LUMO bands of the polyenes in the copolymers consisted of a series of peaks associated with the different vibronic states of the LUMO.[48,51] These peaks are commonly referred to as vibronic fingers.

In the case of samples **6–13**, the distribution could not be determined due to a lack of absolute extinction coefficient data on alternating isomers of polyenes. For samples **4t–13t**, we modeled the spectra of a series of hypothetical all-trans polynorbornene-capped polyenes using Knoll's spectra data of a series of all-trans *tert*-butyl-capped polyenes.[46] The work of Knoll provided the maximum extinction coefficients for the (0–0), (0–1), and (0–2) vibronic fingers of the $\pi\pi^*$ transition of *tert*-butyl-capped 8-ene and 9-ene in methylene chloride, as well as the absorption maxima and relative extinction coefficients of the (0–0), (0–1), (0–2), and (0–3) vibronic fingers of 4–11- and 13-enes in pentane.[44]

A direct application of the extinction coefficient data of the *tert*-butyl-capped polyenes to determine the concentration of polynorbornene-capped-polyenes in the identical solvent was not possible because of hyperconjugation (the contribution of the α-CH molecular orbital to the polyene π electron conjugation) in the polynorbornene-capped polyenes. The difference caused by hyperconjugation was circumvented by measuring the spectra of the copolymers in THF instead of methylene chloride. Because THF has a smaller dielectric constant than methylene chloride, the spectrum of a polyene in THF will be blue shifted relative to its spectrum in methylene chloride.[52] The UV/vis absorption peaks of the *tert*-butyl-capped polyenes in methylene chloride and of the copolymers containing polyenes in THF occurred at identical wavelengths, showing that the solvent-induced blue shift offset the red shift caused by the hyperconjugation effect. Because the *tert*-butyl-capped polyenes in methylene chloride and the copolymers containing polyenes in THF had identical wavelengths at maximum absorption, it was assumed that their maximum extinction coefficients in the respective solvents also would be equivalent. Furthermore, it was assumed that the relative extinction coefficients of the vibronic fingers in a given absorption band would be the same regardless of the solvent. Therefore, Knoll's data on the relative extinction coefficieents of the (0–1), (0–2), and (0–3) vibronic fingers of *tert*-butyl-capped polyenes in pentane were applied directly to the hypothetical polynorbornene-capped polyenes in THF. A quadratic fit of the relative extinction coefficients versus conjugation length was used to determine values for the relative extinction coefficients of the polyenes that Knoll did not examine. Finally, it was necessary to use a convenient relationship for the dependence of the maximum extinction coefficient of the (0–0) vibronic finger on conjugation length. The extinction coefficient is proportional to the square of the transition dipole, and previous research has shown that the dependence of the transition dipole on the conjugation length can be better fit by an inverse dependence on conjugation length than by a linear dependence.[53] Whether or not the inverse relationship directly applies to the (0–0) finger is debatable because the Franck–Condon effect[54] will alter the (0–0) absorption relative to the absorption of the higher order vibronic fingers. However, in this work we found that it was sufficiently accurate to use an

---

(51) Zechmeister, L.; Pinckard, J. H. *J. Am. Chem. Soc.* **1954**, *76*, 4144.

(52) Andersson, P. I.; Gillbro, T.; Ferguson, L.; Cogdell, R. J. *Photochem. Photobiol.* **1991**, *54*, 353.

(53) Kohler, B. E.; Pescatore, J. A. J. In *Conjugated Polymeric Materials: Opportunities in Electronics, Optoelectronics, and Molecular Electronics*; Bredas, J. L., Chance, R. R., Eds.; Kluwer Academic Publishers: Dordrecht, 1990; p 353.

(54) Jaffe, H. H.; Orchin, M. *Theory and Applications of Ultraviolet Spectroscopy*, 2nd ed.; John Wiley and Sons, Inc.: New York, 1962; p 134.

inverse square root dependence of the (0–0) maximum extinction coefficient on conjugation length.

The model spectrum of each polynorbornene-capped polyene was derived empirically from Knoll's data, the preceding assumptions, and the spectra of the copolymers. The model of the absorbance A_N of an N-ene consisted of a summation of four Gaussians corresponding to the (0–0), (0–1), (0–2), and (0–3) vibronic fingers of the $\pi\pi^*$ transition:

$$A_N(\lambda) = \sum_{i=1}^{4} \epsilon_{N,i} \exp\left(-\frac{(\lambda - \lambda_{N,i})^2}{w_N}\right) \qquad (8)$$

The height of the ith Gaussian peak within the summation for a specific N-ene was weighted by its relative extinction coefficient, $\epsilon_{N,i}$, at the wavelength of maximum absorption, $\lambda_{N,i}$. The width of the vibronic fingers was determined by w_N. A single value of w_N for all of the vibronic fingers of a given N-ene was found to be sufficient to fit the polyene and copolymer spectra. The values for w_4, w_5, and w_{13} were determined from the copolymer spectra. The 13(0–0) peak in the spectrum of **13t** was sufficiently distinct to permit an estimation of w_{13}. The remaining w_N were calculated from a linear fit of these values with respect to conjugation length. The $\lambda_{N,i}$ values for the $\pi\pi^*$ (0–0) transitions of all of the polyenes and the $\pi\pi^*$ (0–1) and (0–2) transitions of the polyenes shorter than 12-ene were determined directly from the spectra of the copolymers. The $\lambda_{N,i}$ values for the $\pi\pi^*$ (0–1) or $\pi\pi^*$ (0–2) transitions for the polyenes longer than 11-ene were determined from linear fits of inverse conjugation length to the energy difference between the $\pi\pi^*$ (0–1) and (0–0) transitions or between the $\pi\pi^*$ (0–2) and (0–1) transitions, respectively, in Knoll's data. The $\lambda_{N,i}$ values for the $\pi\pi^*$ (0–3) transition were determined by adding 1340 cm^{-1}, the average energy difference between the two vibronic fingers in Knoll's spectra, to the $\lambda_{N,i}$ values of the $\pi\pi^*$ (0–2) transitions.

Once the parameters were determined for the polyene model spectra, a summation of the polyene models, weighted by $c_{P,N}$, gave the copolymer absorbance A_P:

$$A_P(\lambda) = c_P \sum_{N_{\min}}^{N_{\max}} c_{P,N}\left(\sum_{i=1}^{4} \epsilon_{N,i} \exp\left(-\frac{(\lambda - \lambda_{N,i})^2}{w_N}\right)\right) \qquad (9)$$

$c_P = m_P/\langle M_P\rangle V$, for a mass m_P of copolymer P dissolved in a volume V of solvent. A mean molecular mass $\langle M_P\rangle$ was defined as

$$\langle M_P\rangle = l_P M_{\text{nbe}} + \sum_{N_{\min}}^{N_{\max}} c_{P,N} 26N \qquad (10)$$

where l_P is the length of the polynorbornene blocks and M_{nbe} is the mass of norbornene. The weighted summation accounted for the different polyene lengths. The simplex method[35] was used to minimize the cost function of the square of the difference between $A_P(\lambda)$ and the data, subject to the constraint

$$\sum_{N_{\min}}^{N_{\max}} c_{P,N} = 1 \qquad (11)$$

thereby determining the values of $c_{P,N}$ and l_P.

Hydrolysis of Methylacetoin Ethyl Phosphate. Competing Pathways for Carbonyl Hydrate Participation in a Model for Biotin Carboxylation[†]

Scott D. Taylor and Ronald Kluger*

Contribution from the Lash Miller Laboratories, Department of Chemistry, University of Toronto, Toronto, Ontario, Canada M5S 1A1. Received August 27, 1992

Abstract: Methylacetoin ethyl phosphate (**1**) is a phosphodiester with a carbonyl group β to phosphorus. The phosphate ester of a carbonyl hydrate, expected to be generated from an intramolecular reaction of **1** in base, is a model for an enzymic reaction intermediate which would form from the reaction of the tetrahedral addition production of biotin and bicarbonate with ATP. The hydrolysis of **1** is 10^4–10^5 times more rapid than that of dimethyl phosphate, extrapolated to common conditions (1 M NaOH, 55 °C). Kinetic, product, and isotope labeling studies show that the hydrate of the carbonyl group of **1** serves as an intramolecular nucleophile toward phosphorus, forming the expected phosphate ester of the carbonyl hydrate through cyclic phosphorane intermediates. These adducts decompose by routes which parallel the proposed enzymic mechanism. In addition, solvent isotope incorporation reveals a route not found in reactions of carbonyl-substituted phosphotriesters: the conjugate base of the carbonyl hydrate acts an intramolecular nucleophile at the adjacent carbon atom, forming an unstable hydroxyoxirane (which becomes methylacetoin) and ethyl phosphate. An analogous reaction of ribonucleic acids (and RNAzymes) would have the 2′ hydroxyl group react at the 3′ carbon to form an oxyoxirane, cleaving the 3′ internucleotide bond.

Alkyl diesters of phosphoric acid normally are highly resistant to hydrolysis in neutral aqueous solutions. For example, the estimated half-life for hydrolysis of the phosphate ester linkage in DNA at physiological pH is on the order of millions of years.[1] This high kinetic barrier exists despite a thermodynamic situation which favors hydrolysis.[1] Thus, where catalytic pathways are available, rates of reaction can increase markedly. The primary mechanisms leading to higher spontaneous rates of hydrolysis involve nucleophilic participation at phosphorus by neighboring groups to form reactive five-membered ring intermediates.[2,3] These pathways are characterized by cleavage of the P–O ester bond. Alternative mechanisms involving C–O ester cleavage (participation at carbon with a phosphomonoester leaving group) are much less common.[4-6]

We recently reported studies of the mechanism of acceleration of phosphotriester hydrolysis by neighboring carbonyl groups.[7]

[†] This is paper is dedicated to Professor Frank Westheimer on the occasion of his 80th birthday.

(1) Westheimer, F. H. *Science* **1987**, *235*, 1173.
(2) Thatcher, G. R. J.; Kluger, R. *Adv. Phys. Org. Chem.* **1989**, *25*, 99.
(3) Westheimer, F. H. *Acc. Chem. Res.* **1968**, *1*, 70.
(4) Cox, J. R.; Ramsay, B. *Chem. Rev.* **1964**, *64*, 317.
(5) Brown, D. M.; Magrath, D. I.; Todd, A. R. *J. Chem. Soc.* **1952**, *52*, 2708.
(6) Brown, D. M.; Usher, D. A. *Proc. Chem. Soc.* **1963**, 309.
(7) Kluger, R.; Taylor, S. D. *J. Am. Chem. Soc.* **1991**, *113*, 996.

0002-7863/93/1515-867$04.00/0